doi:10.1038/nature12203

Stability of active mantle upwelling revealed by net characteristics of plate tectonics

Clinton P. Conrad[1], Bernhard Steinberger[2,3] & Trond H. Torsvik[3,4,5]

Viscous convection within the mantle is linked to tectonic plate motions[1–3] and deforms Earth's surface across wide areas[4–6]. Such close links between surface geology and deep mantle dynamics presumably operated throughout Earth's history, but are difficult to investigate for past times because the history of mantle flow is poorly known[7]. Here we show that the time dependence of global-scale mantle flow can be deduced from the net behaviour of surface plate motions. In particular, we tracked the geographic locations of net convergence and divergence for harmonic degrees 1 and 2 by computing the dipole and quadrupole moments of plate motions from tectonic reconstructions[8,9] extended back to the early Mesozoic era. For present-day plate motions, we find dipole convergence in eastern Asia and quadrupole divergence in both central Africa and the central Pacific. These orientations are nearly identical to the dipole and quadrupole orientations of underlying mantle flow, which indicates that these 'net characteristics' of plate motions reveal deeper flow patterns. The positions of quadrupole divergence have not moved significantly during the past 250 million years, which suggests long-term stability of mantle upwelling beneath Africa and the Pacific Ocean. These upwelling locations are positioned above two compositionally and seismologically distinct[10] regions of the lowermost mantle, which may organize global mantle flow[11] as they remain stationary over geologic time[12].

Viscous convection of Earth's mantle dissipates our planet's internal heat, and, because it mobilizes Earth's surface, it is ultimately responsible for the Earth's long history of intense geological activity. Indeed, supercontinent formation and destruction[13], epeirogeny[4,5], mountain-building[6], intraplate volcanism[12] and plate tectonic motions[1–3] have been linked directly to viscous flow in the mantle. Yet, despite these close links, the outlines of present-day global mantle flow have only recently become delineated using tomographic images of the mantle's heterogeneous density structure to inform viscous flow modelling of the mantle[6,14]. Even this has been complicated by the uncertain interpretation of mantle tomography, especially concerning the role of two large low shear-wave velocity provinces (LLSVPs) observed in the lowermost mantle beneath Africa and the Pacific Ocean[15]. Active upwelling from these regions helps to explain patterns of seismic anisotropy[14], plate motions[3], orogeny[5,6] and long-wavelength topography[4], but seismological constraints suggest that these regions are compositionally dense[16–18]. Under these conditions, thermochemical convection can help explain the geometry of upwellings[19], but their stability depends on the interaction of the LLSVP regions with mantle flow[20]. Our knowledge of mantle flow patterns is even poorer for past times, because direct geologic constraints on flow are few and past mantle-density heterogeneity can only be inferred from time-reversed flow models[21] or inverse methods[22] based on present-day mantle structure, or subduction models that do not include active mantle upwelling[1].

Because they are ultimately linked to mantle convection, plate motions should contain information about the underlying mantle flow patterns. Indeed, shear tractions exerted by mantle flow on the lithospheric base may be a primary driver of plate motions[1–3] and thus directly link surface tectonics to interior dynamics. We can exploit this link for past times by using tectonic reconstructions of plate motions, which are becoming increasingly better constrained[8,9], to infer patterns of past mantle flow. We achieve this by examining the net properties of plate motions, which should reflect the 'average' response of Earth's lithosphere to long-wavelength viscous mantle flow. Net rotation of the lithosphere (Fig. 1a) has previously been linked to present-day mantle flow[14], but its utility for past times[8] may be limited because observations of net rotation are highly dependent on the choice of mantle reference frame. By contrast, the relative motions between plates are less dependent on reference frame and are of larger amplitude than net rotation rates. To exploit these attributes, we define several new metrics of relative plate motions that are useful for constraining the interaction

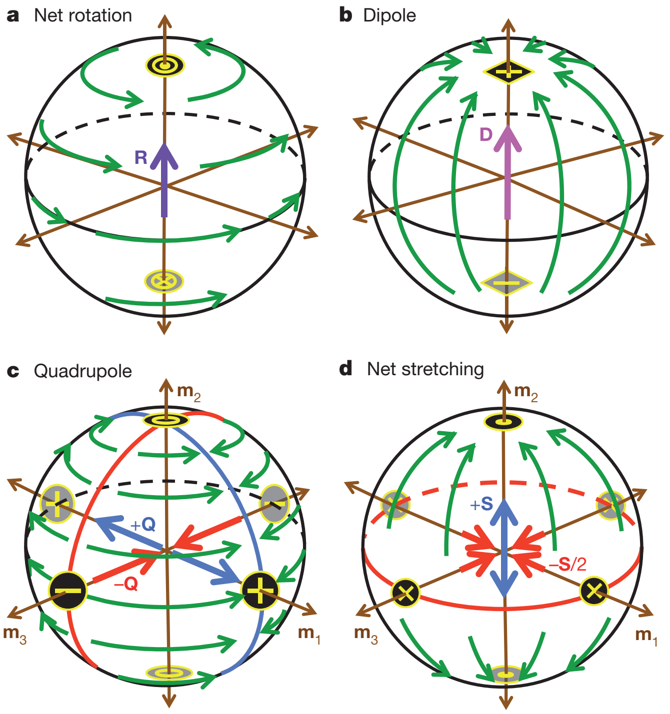

Figure 1 | Definitions of net characteristics. Plate motions for net rotation (**a**), net dipole (**b**), net quadrupole (**c**), and net stretching (**d**) (green arrows; see Supplementary Fig. 2), and their net characteristic vector definitions (**R**, **D**, ±**Q** and +**S**, respectively, and the $\mathbf{m}_1$, $\mathbf{m}_2$ and $\mathbf{m}_3$ eigenvectors; see Methods) are shown. The symbols used to denote pole locations are an encircled dot or cross for positive or negative net rotation poles (**a**), plus or minus within a diamond for positive or negative dipoles (**b**), plus, circle or minus signs within a circle for positive, null, or negative quadrupoles (**c**) and dots or crosses for compressive or extensional net stretching poles (**d**).

[1]Department of Geology and Geophysics, SOEST, University of Hawaii at Mānoa, Honolulu, Hawaii 96822, USA. [2]Helmholtz Centre Potsdam, GFZ German Research Centre for Geosciences, 14473 Potsdam, Germany. [3]Centre for Earth Evolution and Dynamics (CEED), University of Oslo, 0316 Oslo, Norway. [4]Geodynamics, Geological Survey of Norway, NO-7491, Trondheim, Norway. [5]School of Geosciences, University of Witwatersrand, WITS 2050, Johannesburg, South Africa.

between plate tectonics and mantle flow, and apply them to published reconstructions of plate motions both for present and past times.

We defined three new 'net characteristics' of plate motions by performing different integrations of the tectonic plate motion vector field over the surface of the Earth (see Methods). The plate tectonic dipole vector **D** defines a 'net convergence pole' towards which plates are moving in an average sense away from an antipodal 'net divergence pole' (Fig. 1b). The plate tectonic quadrupole, defined by the quadrupole deformation matrix **Q** (see Methods), describes a second-order pattern of net plate motions associated with net hemispheric convergence towards two antipodal 'positive' poles and divergence away from two antipodal 'negative' poles located 90° away from the positive quadrupoles (Fig. 1c). This quadrupole motion occurs as revolution about two intermediate null poles (Fig. 1c). Plate tectonic net stretching, defined by deformation matrix **S** (see Methods), describes convergence towards the two null poles of the quadrupole and divergence away from an equator midway between them (Fig. 1d). These net characteristics describe plate motions at the largest scales; they are influenced by both rapid regional-scale (for example, northwestern North American convergence) and gradual global-scale deformations (for example, the circum-Africa ridge system), but are dominated by the longest-wavelength large-amplitude deformations.

We computed these net characteristics for present-day plate motions (Fig. 2a) and for vector fields associated with two major plate-driving forces: slab pull and basal shear tractions (Fig. 2b). The relevant pole locations for all three net characteristics (**D**, **Q** and **S**) are approximately co-located for both plate motions and plate-driving forces. For example, dipole convergence of plate tectonics occurs in eastern Asia, dominated by convergent motion of the Pacific, Australian, Indian, African and Eurasian plates towards this location (Fig. 2a). The fact that slab pull also converges on average towards this location (Fig. 2b) is perhaps not surprising because subduction results from plate convergence. The convergence of basal tractions towards eastern Asia (Fig. 2b), however, reflects net motion of sub-lithospheric mantle flow towards this region. Within the mantle, downwelling occurs in this location (Fig. 2c), facilitated by a long history of subduction in the western Pacific that is observed tomographically[23]. The co-location of these dipoles thus not only indicates the importance of basal tractions for driving plate motions[1,3], but also illustrates a direct link between plate motions and global-scale patterns of mantle flow.

The quadrupole moments for plate motions, slab pull and basal tractions are also aligned together (Fig. 2). In particular, quadrupole convergence for all three vector fields is centred in the western Pacific and South America (Fig. 2a), near regions of subduction and above major mantle downwellings (Fig. 2c). Similarly, quadrupole divergence is found in the central Pacific and eastern Africa (Fig. 2a, b), above major upwelling regions of the mantle (Fig. 2c) and just east of the location of the LLSVPs in the lowermost mantle (Fig. 2a). Poles orienting (negative) net stretching are also co-located near the geographic poles (Fig. 2a, b), which reflects the equatorial locations of the quadrupoles. As for the dipole, this co-location of quadrupoles reveals the direct link between surface plate motions and mantle flow patterns at depth. If we assume that this link also persisted for alternative plate configurations that existed in the past, then we can use dipole and quadrupole orientations computed for reconstructed past plate motions to infer the large-scale geometry of ancient mantle flow patterns.

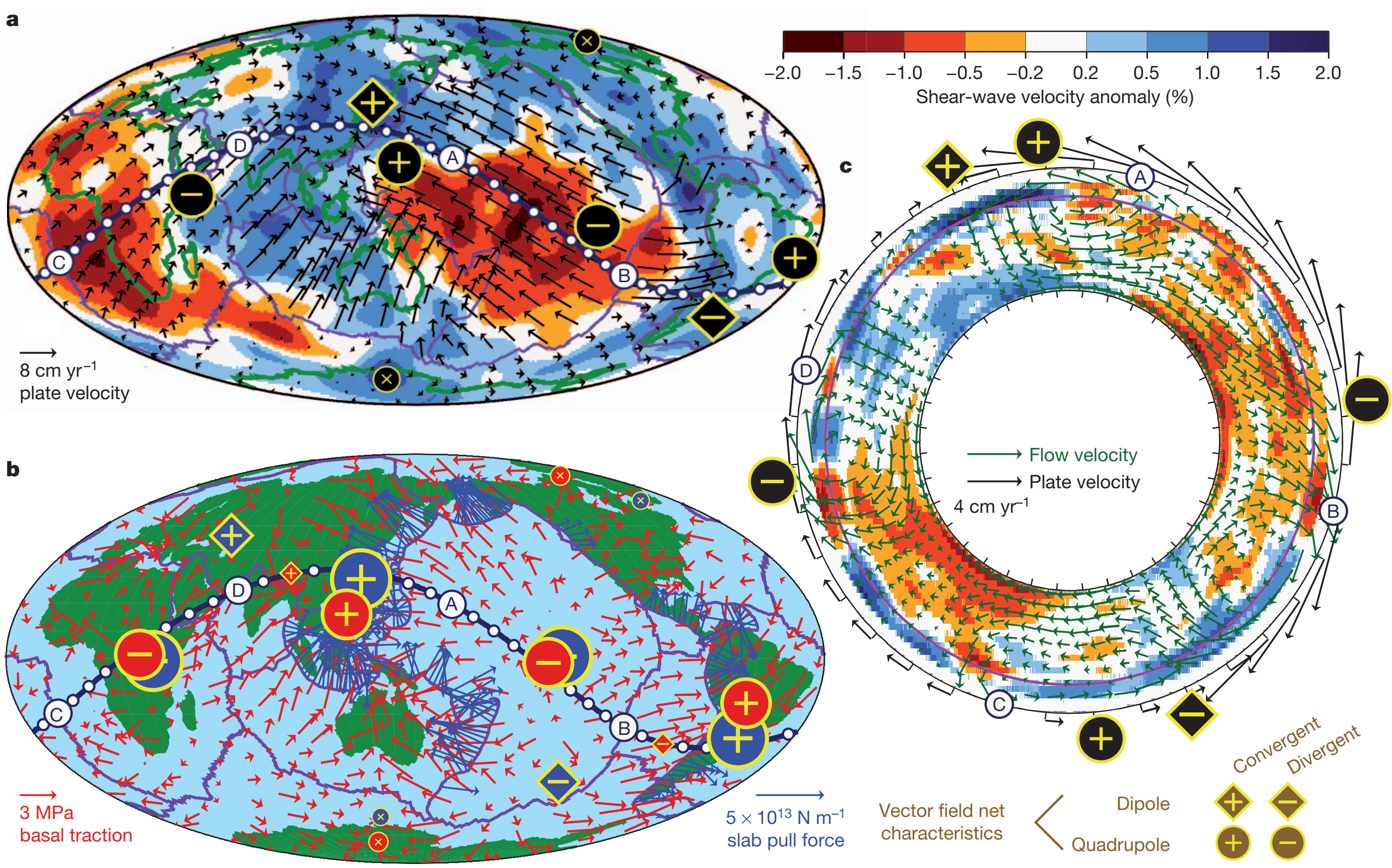

Figure 2 | Association of plate tectonic net characteristics with those of underlying mantle flow. **a**, **b**, Net characteristic pole locations (symbols as in Fig. 1) for the dipole, quadrupole and net stretching components of present-day surface plate motions[28] (black symbols) (**a**) and for plate tectonic driving forces associated with slab pull[29] (blue symbols) and basal tractions on plates[30] (red symbols) (**b**). **c**, A mantle cross-section cutting through great circle ABCD (drawn on maps in all panels) shows the tomographic shear velocity anomaly[23] (colours, also drawn in map view in **a** at 2,800 km depth), the associated mantle flow field[14] (green arrows), surface plate motion (black arrows), and net characteristic dipole and quadrupole locations for plate motions (black symbols).

To determine how dipole and quadrupole orientations have changed during Earth's recent history, we computed **D** and **Q** from a tectonic reconstruction of global plate motions for the past 150 million years (Myr) (ref. 8) that we have extended back to 250 Myr ago by combining palaeomagnetic constraints on absolute and relative plate motions in the African hemisphere[24,25] with a reconstruction of the Pacific basin[9]. The latter is largely synthetic (and thus uncertain) because all Triassic sea floor and any Jurassic hotspot tracks for the Pacific have been lost to subduction. Nevertheless, since 250 Myr ago dipole convergence has generally remained near eastern Asia (Fig. 3a), reflecting the long-term stability of major downwelling beneath this area. Indeed, the stationary position of the Eurasian continent has been noted[26], and is consistent with persistent downwelling of slabs from the adjacent Panthalassa Ocean. The central Pacific and eastern Africa positions of quadrupole divergence have also remained stable above the eastern edges of the LLSVPs (Fig. 3b), which is consistent with the long-term stability of upwelling in these areas. In contrast, the locations of quadrupole convergence have circumscribed Panthalassa, finally resting along its northwestern (and southeastern) edges during the late Cretaceous period (Fig. 3b), about the time that subduction of increasingly younger lithosphere in the northern Pacific[9] may have diminished downwelling flow beneath this region. While migration of the convergent quadrupoles reflects changes in the dominant location of subduction-induced downwelling flow, the stationary nature of the divergent quadrupoles reflects stability of the two major mantle upwellings.

The positioning of mantle upwelling above the African and Pacific LLSVP regions of the lowermost mantle is consistent with flow patterns observed in thermochemical convection models[19]. Our observation that these upwellings have remained stably positioned above the current LLSVP regions may indicate that these LLSVPs form stable 'anchors' that organize mantle flow and surface tectonics[11]. Indeed, plume ascent from the edges of the LLSVPs[12,20] has been used to define an absolute reference frame for plate motions[8] that allows palaeogeography to be reconstructed into the deep past[24]. Our observation of quadrupole stability indicates that the two LLSVP regions have remained separate and in their current locations since at least the beginning of the Mesozoic era, and were not forced into these locations by flow patterns governed by supercontinental surface tectonics since then[27]. Thus, if a transition from degree-1 to degree-2 convection occurred after the formation of Pangea[7] (that is, after about 320 Myr ago), it probably occurred before about 250 Myr ago. The dipole and quadrupole amplitudes (Supplementary Fig. 3) have been decreasing slowly and in concert since the mid-Mesozoic and do not exhibit evidence of a transition between dominant modes (Supplementary Fig. 3). Dipole and quadrupole locations are also rarely co-located (Fig. 3 and Supplementary Fig. 6), which suggests that coupling between the two systems tends to suppress degree-1 upwelling in the vicinity of degree-2 downwelling. Instead, persistent degree-2 upwelling arising from the two LLSVP structures may induce convergent flow in the lowermost mantle that consolidates these structures into their current geometries[20], thus protecting and isolating them over geological timescales[19]. The surface expression of this flow pattern is recorded in the geologic record of plate tectonics.

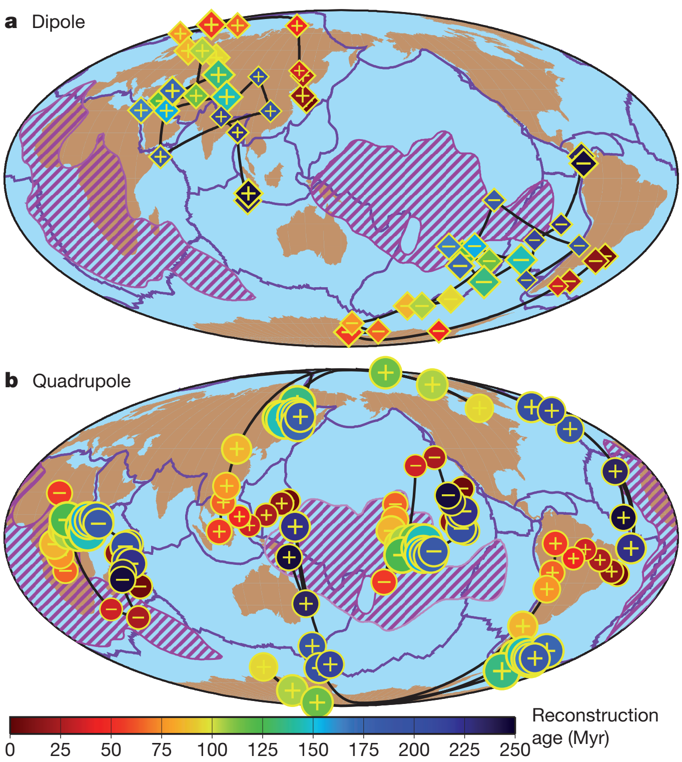

Figure 3 | Temporal evolution of plate tectonic net characteristics. **a**, **b**, Plate tectonic dipole (**a**) and quadrupole (**b**) locations as a function of age for a reconstruction of plate motions since the Triassic period (Supplementary Fig. 6). Symbols as in Fig. 1, with colours indicating reconstruction age and sizes indicating dipole or quadrupole magnitude (Supplementary Fig. 3). Notice the stability of the plate tectonic dipole near eastern Asia (**a**) and the divergent (negative) quadrupole above the eastern edges of the two LLSVPs (denoted here as pink hatching showing where shear waves at 2,800 km are >1% slow[12]) beneath Africa and the Pacific (**b**). Alternative reconstructions[9] (Supplementary Figs 4 and 5) show similar stability of these features.

METHODS SUMMARY

Dipole. We define the 'plate tectonic dipole' **D** as the direct integration of the plate motion velocity field **v** over the Earth's surface A_0 (Supplementary Fig. 1):

$$\mathbf{D} = \frac{3}{2A_0}\int_{A_0} \mathbf{v}\,\mathrm{d}A \qquad (1)$$

Here the normalization is chosen (see Supplementary Information) so that the amplitude of **D** represents the magnitude of motion of the 'pure' dipole on the equator midway between the positive and negative dipole locations (Supplementary Fig. 2b).

Quadrupole and net stretching. Higher-order net characteristics can be computed by integrating the outer product of the unit normal vector $\hat{\mathbf{r}}$ and **v** (Supplementary Fig. 1), and separating the resulting tensor **L** into symmetric (**M**) and antisymmetric (**N**) components:

$$\mathbf{M} + \mathbf{N} = \mathbf{L} = \frac{1}{A_0}\int_{A_0} \hat{\mathbf{r}}\otimes\mathbf{v}\,\mathrm{d}A \qquad (2)$$

Note that the diagonal components of **L** always sum to zero because $\mathrm{tr}(\mathbf{L}) = \frac{1}{A_0}\int_{A_0} \hat{\mathbf{r}}\cdot\mathbf{v}\,\mathrm{d}A$ and $\hat{\mathbf{r}}\perp\mathbf{v}$ everywhere (Supplementary Fig. 1). The three independent components of **N** form the net rotation vector according to $R_k = 3N_{ij}\varepsilon_{ijk}/2$ (see Supplementary Information). The three eigenvalues of the symmetric **M** matrix ($\mu_1 > \mu_2 > \mu_3$) form the diagonalized matrix $\mathbf{M}_\mathrm{D}$, which is simply **M** expressed in a coordinate system defined by the corresponding eigenvectors $\mathbf{m}_1$, $\mathbf{m}_2$, and $\mathbf{m}_3$. We can decompose $\mathbf{M}_\mathrm{D}$ into 'quadrupole' (**Q**) and 'net stretching' (**S**) matrices as:

$$\mathbf{M}_D = \begin{pmatrix} \mu_1 & 0 & 0 \\ 0 & \mu_2 & 0 \\ 0 & 0 & \mu_3 \end{pmatrix} = \frac{\mathbf{Q}}{6} + \frac{4\mathbf{S}}{15}$$
$$= \frac{1}{6}\begin{pmatrix} Q & 0 & 0 \\ 0 & 0 & 0 \\ 0 & 0 & -Q \end{pmatrix} + \frac{4}{15}\begin{pmatrix} -S/2 & 0 & 0 \\ 0 & S & 0 \\ 0 & 0 & -S/2 \end{pmatrix} \qquad (3)$$

where the positive and negative elements of **Q** correspond to eigenvectors $\mathbf{m}_1$ and $\mathbf{m}_3$ respectively (Fig. 1c), and the unique (middle) element of **S** corresponds to eigenvector $\mathbf{m}_2$ (Fig. 1d). The piercing points of the eigenvectors $\pm\mathbf{m}_1$, $\pm\mathbf{m}_2$ and $\pm\mathbf{m}_3$ thus define the positive (convergent) quadrupoles, the net stretching poles (also null quadrupoles), and the negative (divergent) quadrupoles, respectively

(Fig. 1c and 1d). We have defined $Q = 6\mu_1 + 3\mu_2$ and $S = 15\mu_2/4$ so that these values correspond to the maximum velocity magnitudes within the 'pure' quadrupole and net stretching velocity fields (see Supplementary Information). Note that the net stretching deformation (Fig. 1d) reverses to become 'net flattening' (polar extension and equatorial compression) if $S < 0$ ($\mu_2 < 0$).

Received 13 November 2012; accepted 18 April 2013.

1. Lithgow-Bertelloni, C. & Richards, M. A. The dynamics of Cenozoic and Mesozoic plate motions. *Rev. Geophys.* **36,** 27–78 (1998).
2. Stadler, G. *et al.* The dynamics of plate tectonics and mantle flow: from local to global scales. *Science* **329,** 1033–1038 (2010).
3. van Summeren, J., Conrad, C. P. & Lithgow-Bertelloni, C. The importance of slab pull and a global asthenosphere to plate motions. *Geochem. Geophys. Geosyst.* **13,** Q0AK03 (2012).
4. Lithgow-Bertelloni, C. & Silver, P. G. Dynamic topography, plate driving forces and the African superswell. *Nature* **395,** 269–272 (1998).
5. Flowers, R. M., Ault, A. K., Kelley, S. A., Zhang, N. & Zhong, S. J. Epeirogeny or eustasy? Paleozoic-Mesozoic vertical motion of the North American continental interior from thermochronometry and implications for mantle dynamics. *Earth Planet. Sci. Lett.* **317–318,** 436–445 (2012).
6. Becker, T. W. & Faccenna, C. Mantle conveyor beneath the Tethyan collisional belt. *Earth Planet. Sci. Lett.* **310,** 453–461 (2011).
7. Zhang, N., Zhong, S. J., Leng, W. & Li, Z. X. A model for the evolution of the Earth's mantle structure since the Early Paleozoic. *J. Geophys. Res. Solid Earth* **115,** B06401 (2010).
8. Torsvik, T. H., Steinberger, B., Gurnis, M. & Gaina, C. Plate tectonics and net lithosphere rotation over the past 150 My. *Earth Planet. Sci. Lett.* **291,** 106–112 (2010).
9. Seton, M. *et al.* Global continental and ocean basin reconstructions since 200 Ma. *Earth Sci. Rev.* **113,** 212–270 (2012).
10. Garnero, E. J. & McNamara, A. K. Structure and dynamics of Earth's lower mantle. *Science* **320,** 626–628 (2008).
11. Dziewonski, A. M., Lekic, V. & Romanowicz, B. A. Mantle anchor structure: an argument for bottom up tectonics. *Earth Planet. Sci. Lett.* **299,** 69–79 (2010).
12. Torsvik, T. H., Smethurst, M. A., Burke, K. & Steinberger, B. Large igneous provinces generated from the margins of the large low-velocity provinces in the deep mantle. *Geophys. J. Int.* **167,** 1447–1460 (2006).
13. Li, Z.-X. & Zhong, S. Supercontinent–superplume coupling, true polar wander and plume mobility: plate dominance in whole-mantle tectonics. *Phys. Earth Planet. Inter.* **176,** 143–156 (2009).
14. Conrad, C. P. & Behn, M. D. Constraints on lithosphere net rotation and asthenospheric viscosity from global mantle flow models and seismic anisotropy. *Geochem. Geophys. Geosyst.* **11,** Q05W05 (2010).
15. Lassak, T. M., McNamara, A. K., Garnero, E. J. & Zhong, S. J. Core-mantle boundary topography as a possible constraint on lower mantle chemistry and dynamics. *Earth Planet. Sci. Lett.* **289,** 232–241 (2010).
16. Kennett, B. L. N., Widiyantoro, S. & van der Hilst, R. D. Joint seismic tomography for bulk sound and shear wave speed in the Earth's mantle. *J. Geophys. Res.* **103,** 12469–12493 (1998).
17. Ishii, M. & Tromp, J. Normal-mode and free-air gravity constraints on lateral variations in velocity and density of Earth's mantle. *Science* **285,** 1231–1236 (1999).
18. Deschamps, F. & Trampert, J. Mantle tomography and its relation to temperature and composition. *Phys. Earth Planet. Inter.* **140,** 277–291 (2003).
19. McNamara, A. K., Garnero, E. J. & Rost, S. Tracking deep mantle reservoirs with ultra-low velocity zones. *Earth Planet. Sci. Lett.* **299,** 1–9 (2010).
20. Bower, D. J., Gurnis, M. & Seton, M. Lower mantle structure from paleogeographically constrained dynamic Earth models. *Geochem. Geophys. Geosyst.* **14,** 44–63 (2013).
21. Steinberger, B. & O'Connell, R. J. Changes of the Earth's rotation axis owing to advection of mantle density heterogeneities. *Nature* **387,** 169–173 (1997).
22. Liu, L. J., Spasojevic, S. & Gurnis, M. Reconstructing Farallon Plate subduction beneath North America back to the Late Cretaceous. *Science* **322,** 934–938 (2008).
23. Ritsema, J., van Heijst, H. J. & Woodhouse, J. H. Global transition zone tomography. *J. Geophys. Res.* **109,** B02302 (2004).
24. Torsvik, T. H., Müller, R. D., Van der Voo, R., Steinberger, B. & Gaina, C. Global plate motion frames: toward a unified model. *Rev. Geophys.* **46,** RG3004 (2008).
25. Steinberger, B. & Torsvik, T. H. Absolute plate motions and true polar wander in the absence of hotspot tracks. *Nature* **452,** 620–623 (2008).
26. Collins, W. J. Slab pull, mantle convection, and Pangaean assembly and dispersal. *Earth Planet. Sci. Lett.* **205,** 225–237 (2003).
27. Zhong, S. J., Zhang, N., Li, Z. X. & Roberts, J. H. Supercontinent cycles, true polar wander, and very long-wavelength mantle convection. *Earth Planet. Sci. Lett.* **261,** 551–564 (2007).
28. DeMets, C., Gordon, R. G., Argus, D. F. & Stein, S. Effect of recent revisions to the geomagnetic reversal time scale on estimates of current plate motions. *Geophys. Res. Lett.* **21,** 2191–2194 (1994).
29. Wu, B. J., Conrad, C. P., Heuret, A., Lithgow-Bertelloni, C. & Lallemand, S. Reconciling strong slab pull and weak plate bending: the plate motion constraint on the strength of mantle slabs. *Earth Planet. Sci. Lett.* **272,** 412–421 (2008).
30. Naliboff, J. B., Conrad, C. P. & Lithgow-Bertelloni, C. Modification of the lithospheric stress field by lateral variations in plate-mantle coupling. *Geophys. Res. Lett.* **36,** L22307 (2009).

Supplementary Information is available in the online version of the paper.

Acknowledgements We are grateful for NSF CAREER grant EAR-1151241 (to C.P.C.) and ERC grant 267631 (to T.H.T.), and to the Norwegian Centre for Advanced Study in Oslo for making this collaboration possible.

Author Contributions C.P.C. defined the method to compute net characteristics, B.S. and T.H.T. extended the plate reconstruction through the Mesozoic, all authors developed the geologic application and interpretation and C.P.C. prepared the manuscript with input, comments and review from all authors.

Author Information Reprints and permissions information is available at www.nature.com/reprints. The authors declare no competing financial interests. Readers are welcome to comment on the online version of the paper. Correspondence and requests for materials should be addressed to C.P.C. (clintc@hawaii.edu).